

# Adiabatic Quantum Pumping of Coherent Electrons

Ora ENTIN-WOHLMAN, Amnon AHARONY, and Vyacheslavs KASHCHEYEVS  
*School of Physics and Astronomy, Raymond and Beverly Sackler Faculty of Exact Sciences,  
Tel Aviv University, Tel Aviv 69978, ISRAEL*

Received November 14, 2018

## Abstract

We review recent theoretical calculations of charge transfer through mesoscopic devices in response to slowly-oscillating, spatially-confined, potentials. The discussion is restricted to non-interacting electrons, and emphasizes the role of quantum interference and resonant transmission in producing almost integer values (in units of the electronic charge  $e$ ) of the charge transmitted per cycle,  $Q$ . The expression for the pumped charge is derived from a systematic expansion of the system scattering states in terms of the temporal derivatives of the instantaneous solutions. This yields the effect of the modulating potential on the Landauer formula for the conductance in response to a constant bias on one hand, and the corrections to the widely-used adiabatic-limit formula (in which the modulation frequency is smaller than any electronic relaxation rate) on the other hand. The expression for  $Q$  is used in connection with simple models to exemplify the intimate relationship between resonant transmission through the mesoscopic device and almost integral values of  $Q$ , and to analyze the charge pumped by a surface acoustic wave coupled to a quantum channel by the piezoelectric effect.

**Key Words:** interference in nanostructures, quantum pumping, surface acoustic waves, resonant transmission.

## 1. Introduction

Although electric charge consists of units of the electronic charge  $e$ , the electric current in macroscopic samples is not quantized, but rather behaves as a continuous fluid. The ability to control current on the level of single electrons is feasible in mesoscopic devices, and at low enough temperatures. The theoretical possibility of current quantization has been first addressed by Thouless [1], who considered the direct current (dc) induced in a one-dimensional gas of non-interacting electrons by a slowly-moving periodic potential profile. Thouless has shown that when the Fermi energy lies in the gap between the filled and empty bands of the time-dependent Hamiltonian (and the gap does not close within the cycle), the current transmitted through a cross-section of the sample over a single period  $T$  of the potential corresponds to an integral number of  $e$ :  $I = (e/T) \times \text{integer}$ , where  $T = a/v$ , with  $a$  and  $v$  being the lattice constant of the potential profile and its velocity. The robustness of the quantization in such systems, with respect to the effect of disorder or of many-body interactions, has been further discussed in Refs. [2]. The charge transmitted in this way is independent of the frequency of the modulating potential (and hence the current per period is proportional to the frequency).

The model of Thouless is a remarkably clear example of the phenomenon termed ‘charge pumping’ [3, 4]. Experimentally, investigations of this phenomenon focus on confined nanostructures, e.g., quantum dots, carbon nanotubes, or quantum channels. In the latter, traveling potential profiles, like the one required in the Thouless model, can be generated using the piezo-electric coupling of surface acoustic waves to the two-dimensional electron gas formed in GaAs-AlGaAs heterostructures [5]. Another possibility is to modulate periodically gate voltages applied to quantum-dot devices [6, 7, 8, 9]. Exploiting the Coulomb-blockade

effect, this leads to quantization of the transmitted charge, and is of metrological use [10]. Devices of this type are called ‘single-electron turnstiles’.

Charge pumping is achieved by varying certain parameters of the system Hamiltonian periodically with time. When the change is carried out slowly enough, the Hamiltonian returns to itself after each cycle, and adiabatic control of the electronic states becomes feasible. Under these circumstances, the modulating potential affects predominantly the quantum interference of the electrons in the structure, not their classical trajectories. This situation is called ‘adiabatic quantum pumping’ [11, 12, 13, 14, 15, 16, 17, 18, 19, 20, 21, 22, 23], and necessitates the maintenance of a phase-coherent motion of the electrons (effects of dissipation, inelastic scattering, noise and dephasing on quantum pumping have been discussed in Refs. [24, 25, 26]). Quantum pumping has been realized in an ‘open’ quantum dot under conditions in which Coulomb-blockade effects are not important [27]. The device of Ref. [27] consists of a semi-conductor quantum dot, coupled to electronic reservoirs by ballistic point-contacts. By varying gate voltages, the shape of the confining potential of the electrons in the dot has been modulated periodically, leading to a dc potential difference as a consequence of electronic transfer between reservoirs. The importance of quantum interference in determining the magnitude and direction of the pumped charge has been clearly demonstrated by applying a weak magnetic field perpendicular to the sample [27]. Recently, the possibility of spin-polarized pumped currents has been discussed [28, 29].

Whereas a highly-accurate quantized pumped current has been observed in the turnstile device [7] (in which the quantization is dictated by the Coulomb-blockade effect), this is not the case in the open-dot geometry [27] (where this effect is expected to play a minor role). It is therefore of fundamental interest to study charge pumping of non-interacting electrons resulting from interference effects, to explore the circumstances under which it is optimal [16, 20, 21, 30]. In this context, it is especially useful to investigate simple, tractable models, where it is possible to relate the parameters characterizing the nanostructure, notably the point-contact conductances, with those that govern the magnitude of the pumped charge. Thus by considering a small quantum dot which supports resonant transmission, it has been shown [19, 20] that when the Fermi energy in the leads connecting the dot with the electronic reservoirs aligns with the quasi-bound state energy in the dot, the charge pumped over a period is close to  $e$ .

In the following, the conditions for the charges pumped over a period,  $Q$ , to be (almost) quantized due to interference effects alone will be reviewed. Our discussion begins in Sec. 2 with the derivation of the expression for that charge. The derivation is based on a systematic expansion of the time-dependent scattering states around the instantaneous solution. The first-order yields (when the system is un-biased by constant chemical potential differences) the widely-used ‘adiabatic approximation’, and reproduces the formula of Brouwer [12]. The next order gives the first correction to the adiabatic approximation. We continue (in Sec. 3) with an analysis of the turnstile geometry. That discussion points out to the connection between the conditions for resonance transmission and integral values of  $Q$ . In Sec. 4 we discuss the pump based on the surface acoustic waves (SAW’s), and show that interference effects lead to a staircase structure of the acousto-current driven by the SAW’s, similar to the one observed in the experiments [5]. Finally, Sec. 5 includes concluding remarks.

## 2. Time-dependent Scattering Theory: Adiabatic Expansion

Consider a ballistic nanostructure of arbitrary geometry, connected by an arbitrary number of leads (denoted by  $\alpha$ ) to massive metallic conductors which serve as electron reservoirs (kept at thermal equilibrium). Each reservoir is kept at a chemical potential  $\mu_\alpha$ , such that the electrons in it obey the Fermi distribution

$$f_\alpha(E) = \frac{1}{e^{\beta(E-\mu_\alpha)} + 1}. \quad (1)$$

The nanostructure is also subject to a potential modulated periodically in time,  $V(\mathbf{r}, t)$  which is confined to the structure, such that asymptotic behaviors of the scattering solutions can be defined in an un-ambiguous manner. The Hamiltonian of the system then reads

$$\mathcal{H}(\mathbf{r}, t) = \mathcal{H}_0(\mathbf{r}) + V(\mathbf{r}, t), \quad (2)$$

in which  $\mathcal{H}_0$  consists of the kinetic energy. As in the usual scattering treatment, we seek for the scattering state  $\Psi_{\alpha n}$ , which is excited by the free wave  $w_{\alpha n}^-$  (incoming in the transverse mode  $n$  of lead  $\alpha$  with energy  $E$ ), which is normalized to carry a unit flux,

$$\Psi_{\alpha n}(\mathbf{r}, t) = e^{-iEt} \chi_{\alpha n}(\mathbf{r}, t) \equiv e^{-iEt} \left( w_{\alpha n}^-(\mathbf{r}) + \tilde{\chi}_{\alpha n}(\mathbf{r}, t) \right). \quad (3)$$

By inserting this form into the time-dependent Schrödinger equation, (noting that  $w_{\alpha n}^-$  is an eigenstate of  $\mathcal{H}_0$ ),  $\tilde{\chi}_{\alpha n}$  can be written in terms of the instantaneous Green function,  $G^t(E)$ ,

$$\left( E - \mathcal{H}(\mathbf{r}, t) \right) G^t(E; \mathbf{r}, \mathbf{r}') = \delta(\mathbf{r}' - \mathbf{r}), \quad (4)$$

as follows [31]

$$\left( G^t \right)^{-1} \tilde{\chi}_{\alpha n}(\mathbf{r}, t) = V(\mathbf{r}, t) w_{\alpha n}^-(\mathbf{r}) - i \frac{\partial \tilde{\chi}_{\alpha n}(\mathbf{r}, t)}{\partial t}. \quad (5)$$

Note that the time dependence of the scattered wave function,  $\tilde{\chi}_{\alpha n}(\mathbf{r}, t)$ , has the same characteristic time scale as  $V$ : e.g., when the modulating potential is oscillating in time with frequency  $\omega$ ,  $\tilde{\chi}$  contains all harmonics. Once the time-dependent scattering solution is known, the thermal average of the current density operator is given by [32, 33, 34]

$$\langle \mathbf{j}(\mathbf{r}, t) \rangle = \frac{e}{m} \Im \int \frac{dE}{2\pi} \sum_{\alpha n} f_{\alpha}(E) \chi_{\alpha n}^*(\mathbf{r}, t) \frac{\partial \chi_{\alpha n}(\mathbf{r}, t)}{\partial \mathbf{r}}. \quad (6)$$

Evaluating  $\langle \mathbf{j}(\mathbf{r}, t) \rangle$  as  $\mathbf{r}$  approaches  $\infty$  in lead  $\beta$ , and then integrating over the cross-section of that lead yields the current  $I_{\beta}(t)$  flowing into lead  $\beta$  [31, 34].

The time-dependent scattering solutions are derived from a systematic expansion in the temporal derivatives of the instantaneous solutions (that is, the scattering solutions of the Hamiltonian in which time is ‘frozen’). Namely, Eq. (5) is solved iteratively: the temporal derivative appearing on the right-hand-side is regarded as a small correction. The zero-order,  $\chi_{\alpha n}^t$ , is the scattering solution of the instantaneous Hamiltonian (in which time appears as a parameter),

$$\chi_{\alpha n}^t(\mathbf{r}) = w_{\alpha n}^-(\mathbf{r}) + \int d\mathbf{r}' G^t(E; \mathbf{r}, \mathbf{r}') V(\mathbf{r}', t) w_{\alpha n}^-(\mathbf{r}'). \quad (7)$$

Then the scattering solution reads

$$\chi(\mathbf{r}, t) = \chi^t(\mathbf{r}) + \chi^{(1)}(\mathbf{r}, t) + \chi^{(2)}(\mathbf{r}, t) + \dots, \quad (8)$$

with the first-order

$$\chi^{(1)}(\mathbf{r}, t) = -i \int d\mathbf{r}' G^t(E; \mathbf{r}, \mathbf{r}') \dot{\chi}^t(\mathbf{r}'), \quad (9)$$

and the second-order

$$\chi^{(2)}(\mathbf{r}, t) = -i \int d\mathbf{r}' G^t(E; \mathbf{r}, \mathbf{r}') \Delta \dot{\chi}^t(\mathbf{r}'), \quad (10)$$

where

$$\Delta \dot{\chi}^t(\mathbf{r}') = -i \int d\mathbf{r}'' \frac{d}{dt} \left( G^t(E; \mathbf{r}', \mathbf{r}'') \dot{\chi}^t(\mathbf{r}'') \right), \quad (11)$$

and  $\dot{\chi}_{\alpha n}^t \equiv d\chi_{\alpha n}^t/dt$ . Hence, in our iterative solution, the time-dependent scattering states are given entirely in terms of the *instantaneous* solutions of the problem at hand. This expansion procedure necessitates that the characteristic inverse time-constant, which describes the time dependence of the modulating potential, will be smaller than any characteristic energy scale of the electrons. However, it turns out that the expansion also requires that the amplitude of the modulating potential will be small. In general, the validity regime of the adiabatic expansion is a rather delicate question, being related to the ratio of the time it takes the electrons to traverse the sample (the Wigner time), and the time-constant of the modulating potential [16, 35]. In this respect, the comparison of the results from the adiabatic expansion, and the exact Floquet solution of the problem (when possible), are highly desirable [36].

## 2.1. The Adiabatic Approximation

Let us first analyze the net current passing through the system utilizing the adiabatic approximation, that is, keeping only the term (9). For simplicity, we confine the discussion to a nanostructure connected to left ( $\ell$ ) and right ( $r$ ) leads. Then the current flowing during a single period of the modulating potential is [31]

$$I = \frac{1}{2} \oint \frac{dt}{T} (I_\ell(t) - I_r(t)) = I_{\text{bias}} + I_{\text{pump}}, \quad (12)$$

where  $T$  is the periodicity of the modulating potential. The first part,  $I_{\text{bias}}$ , flows only when the system is biased,

$$I_{\text{bias}} = e \oint \frac{dt}{T} \int \frac{dE}{4\pi} (f_\ell(E) - f_r(E)) \times \sum_{nm} \left[ 2|S_{rm,\ell n}^t|^2 + \Re \left( S_{\ell m,\ell n}^t U_{\ell m,\ell n}^* - S_{\ell m,rn}^t U_{\ell m,rn}^* - S_{rm,\ell n}^t U_{rm,\ell n}^* + S_{rm,rn}^t U_{rm,rn}^* \right) \right], \quad (13)$$

where  $U_{\beta m,\alpha n} = \int d\mathbf{r} \chi_{\beta m}^t(\mathbf{r}) \dot{\chi}_{\alpha n}^t(\mathbf{r})$ , and  $S_{\beta m,\alpha n}^t$  is the matrix element of the instantaneous scattering matrix. Equation (13) can be considered as a generalization of the Landauer formula, extended to include the effect of a time-dependent potential in the adiabatic approximation. The second part of the current,  $I_{\text{pump}}$ , is established by the time-dependent potential (though it is affected by the chemical potential difference, when the latter is applied). Explicitly,

$$I_{\text{pump}} = e \oint \frac{dt}{T} \int \frac{dE}{4\pi} \frac{\partial(f_\ell(E) + f_r(E))}{\partial E} \frac{1}{2} \sum_m \left[ \langle \chi_{\ell m}^t | \dot{V} | \chi_{\ell m}^t \rangle - \langle \chi_{rm}^t | \dot{V} | \chi_{rm}^t \rangle \right]. \quad (14)$$

It can be shown [31] that the terms in the square brackets of (14) reproduce the Brouwer [12] formula, derived for an unbiased system (in which  $I_{\text{pump}}$  is given in terms of temporal derivatives of the instantaneous scattering matrix).

## 2.2. Corrections to the Adiabatic Approximation

When the second-order in the expansion (8) is retained, one obtains the first correction to the widely-used adiabatic approximation. We will discuss here the pumping current beyond the adiabatic approximation for an unbiased system connected to two single-channel leads. In that case, the current entering lead  $\beta$  consists of two parts, the leading order in the adiabatic approximation,  $I_\beta$ , which has been discussed above, and a correction,  $\Delta I_\beta$ . Explicitly [31]

$$\begin{aligned} \tilde{I}_\beta(t) &= I_\beta(t) + \Delta I_\beta(t), \\ I_\beta(t) &= \frac{e}{2\pi} \int dE \left( \frac{\partial f(E)}{\partial E} \right) \langle \chi_\beta^t | \dot{V} | \chi_\beta^t \rangle, \\ \Delta I_\beta(t) &= \Im \left( \langle \chi_\beta^t | 2\dot{V}(t) \dot{G}^t(E) + \ddot{V}(t) G^t(E) | \chi_\beta^t \rangle \right). \end{aligned} \quad (15)$$

The relative magnitude of the correction compared to the leading-order term may be accessed by noting that [31]

$$\begin{aligned} &\langle \chi_\beta^t | 2\dot{V}(t) \dot{G}^t(E) + \ddot{V}(t) G^t(E) | \chi_\beta^t \rangle \\ &= -\langle \chi_\beta^t | 2\dot{V} G^t(E) \dot{V} + \ddot{V} | \frac{\partial \chi_\beta^t}{\partial E} \rangle. \end{aligned} \quad (16)$$

Hence, the validity of the adiabatic approximation is not only restricted by the smallness of the inverse time-constant  $T$  dominating the temporal derivatives. It depends as well on the energy derivatives of the scattering states (i.e., the energy scale of the instantaneous reflection and transmission amplitudes) and the strength of the modulating potential itself [37]. Below, we evaluate the pumping current in the adiabatic approximation, keeping the above restrictions in mind.

### 3. Interference and Quantized Pumping in Turnstile Devices

The correlation between resonant transmission and the magnitude of adiabatically pumped charge may be summarized generically as follows. Consider a quantum dot, connected to its external leads by two point-contacts, whose conductances are controlled by split-gate voltages which are modulated periodically in time. During each cycle the system follows a closed curve, the ‘pumping contour’, in the parameter plane spanned by the point-contact conductances. As the system parameters are varied (for example, the gate voltage on the dot) the pumping contour distorts and shifts, forming a Lissajous curve in the parameter plane. The pumped charge will be (almost) quantized when the pumping contour encircles transmission peak(s) (that is, resonances) of the quantum dot in that parameter plane. Its magnitude (in units of the electronic charge,  $e$ ) and sign are determined by the winding number of the pumping contour.

In order to exemplify this idea, we employ the tight-binding description, and imagine the quantum dot to be coupled to semi-infinite, one-dimensional and single-channel leads by matrix elements  $J_\ell$  and  $J_r$ . Those are oscillating in time with frequency  $\omega$ , such that the modulation amplitude is  $P$  and the phase shift between the  $J_\ell$  modulation and that of  $J_r$  is  $2\phi$ ,

$$J_\ell = J_L + P \cos(\omega t + \phi), \quad J_r = J_L + P \cos(\omega t - \phi). \quad (17)$$

The point-contact conductances are then given (in dimensionless units) by  $X_\ell \equiv J_\ell^2$  and  $X_r \equiv J_r^2$ . As the couplings of the quantum dot to the leads are modulated in time,  $J_\ell$  and  $J_r$  can attain both negative and positive values. This reflects a modulation of the potential shaping the dot: The tight-binding parameters  $J_\ell$  and  $J_r$ , which are derived as integrals over the site ‘atomic’ wave functions and the oscillating potential, can have both signs. The extreme modulation arises for  $J_L = 0$ , when the hopping matrix elements which couple the dot to the leads oscillate in the range  $\{-P, P\}$ . The conductances of the point contacts are then modulated in the range  $\{0, P^2\}$ . The corresponding Lissajous curve of the pumping is then a simple closed curve. Another possibility is to keep the couplings finite at any time, i.e.,  $J_L \neq 0$ , and to modulate the couplings around this value. In that case the Lissajous curve may fold on itself [compare Figs. 2 and 3 below]. This yields a rather rich behavior of the pumped charge.

Indeed, using the expression for the charge,  $Q$ , pumped through the quantum dot during a single period of the modulation (14),

$$Q = \frac{e}{4\pi} \oint dt \left[ \langle \chi_r^t | \dot{V} | \chi_r^t \rangle - \langle \chi_\ell^t | \dot{V} | \chi_\ell^t \rangle \right], \quad (18)$$

(the limit of zero temperature is taken for simplicity) where  $\chi_{\ell,r}^t$  are the instantaneous scattering solutions incited by free waves from the left ( $\ell$ ) and from the right ( $r$ ), the variation of  $Q$  as function of  $P$  is, e.g.,

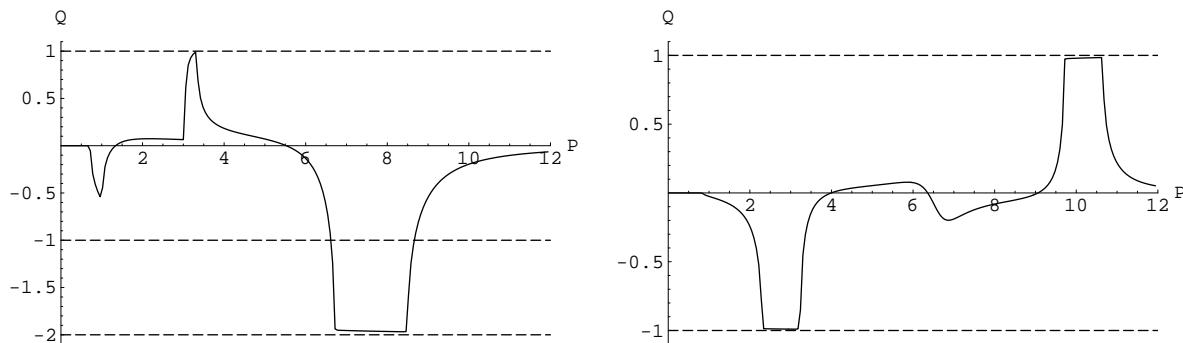


**Figure 1.** The pumped charge,  $Q$ , in units of  $e$ , as function of the modulating amplitude,  $P$ .

(In drawing these figures, we have used a tight-binding description for the entire system, and varied the model parameters, see Ref. [30].)

In order to relate the ‘quantized’ values of  $Q$ , as portrayed for example on the left panel of Fig. 1, and the location of the pumping contour relative to the resonant transmission of the quantum dot, we exhibit in Figs. 2 the pumping contour in the parameter plane, and the resonance lines, for several values of  $P$ .

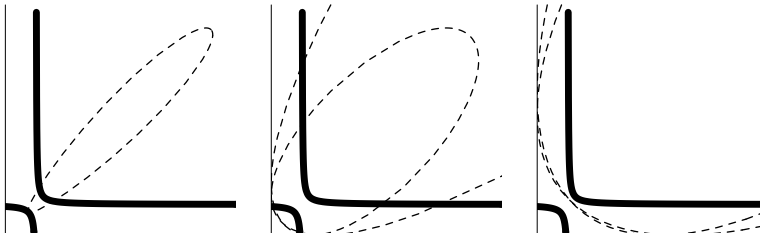


**Figure 2.** The pumping contour (dashed line) and the resonance lines (thick lines), in the  $\{X_\ell - X_r\}$  plane, for  $P=1$ , (left panel),  $P=5$  (central panel) and  $P=8$  (right panel).

The resonance lines are found by calculating the transmission through the quantum dot as function of  $X_\ell$  and  $X_r$ . One then finds [30] that when either  $X_\ell$  or  $X_r$  is varied while the other parameter is kept fixed, the maxima of the transmission occur on two ‘resonance lines’, shown in thick lines in Figs. 2. The figures also show the topology of the curve traversed by the system during the pumping cycle for representative values of  $P$ . When  $P=1$ , the pumping contour encloses a small part of the upper resonance line, and also touches the peak on the lower resonance line. Indeed,  $Q$  has an intermediate value near  $-0.5$ , decreasing to zero as  $P$  moves away from 1 (see Fig. 1, left panel). Increasing the amplitude to the value  $P=5$  reveals that the pumping contour encloses both peaks on the resonance lines, and therefore their separate contributions almost cancel one another, leading to a tiny value of  $Q$ . Also, the pumping curve begins to fold on itself, giving rise to the ‘bubble’ close to the origin (see central and left panels in Fig. 2). Following the increase of that bubble as  $P$  is enhanced leads to the situation in which the bubble encloses the lower resonance, and then the charge attains a unit value (see left panel on Fig. 1). As the bubble increases further, capturing the two resonance lines,  $Q$  again becomes very small. But upon further increasing  $P$ , we reach the interesting situation, depicted in Fig. 2 for  $P=8$ , in which the bubble encircles *twice* the upper resonance line, leading to a pumped charge very close to  $|2e|$  (see left panel on Fig. 1).

Thus, the condition for obtaining integral values of the pumped charge is that the contour traversed by the system in the parameter plane spanned by the pumping parameters should encircle a significant portion of a resonance line in that plane. The magnitude and the sign of the pumped charge are determined by that portion, and by the direction along which the resonance line is encompassed. We emphasize that the pumping contour, as well as the resonance lines, can be determined experimentally [20].

The reason for this topological description of adiabatic charge pumping can be traced back to the expression for the pumped charge, Eq. (18). The main contribution to the temporal integration there comes from the poles of the integrand. The same poles are also responsible for the resonant states of the nanostructure, that is, for the maxima in the transmission coefficient [20, 30]. One can imagine more complex scenarios: Including higher harmonics of  $\omega$  in the time dependence of the point contact conductances can create more complex Lissajous contours, which might encircle portions of the resonance lines more times, yielding higher quantized values of the pumped charge.

Finally, it should be mentioned that the results presented above are obtained at zero temperature. At finite temperatures, the expression for  $Q$  should be integrated over the the electron energy  $E$ , with the Fermi function derivative  $-\partial f/\partial E$ . Hence, upon the increase of the temperature, the pumped charge would be smeared and suppressed. It would be very interesting to check the above predictions in more complicated models (for example, when there are several levels on each of the sites forming the quantum dot), allowing for a richer structure of the transmission in the parameter space, and, of course, in real systems.

## 4. Pumping by Surface Acoustic Waves in a Quantum Channel

Modulation of the potential acting on a nanostructure may be also achieved through the piezoelectric effect of surface acoustic waves (SAW's), which is relatively large in GaAs. In the two-dimensional electron gas formed in GaAs-AlGaAs samples the potential created by the SAW is screened out. However, the SAW's are effective within a quasi-one-dimensional channel (where screening is diminished) defined in GaAs-AlGaAs samples. In the experiments [5], the time-averaged current exhibits steps between plateaus, at quantized values of integer  $\times e(\omega/2\pi)$ , ( $\omega$  is the SAW frequency), as function of either the gate voltage on the quantum channel, or the SAW amplitude. Here we propose an explanation for this observation, in terms of interference of non-interacting electrons [38, 39].

Unlike the turnstile-like case, the piezoelectric potential,  $\mathcal{H}_{\text{SAW}}(\mathbf{r}, t) = P \cos(\omega t - \mathbf{q} \cdot \mathbf{r})$ , generated by the SAW oscillates with time everywhere inside the nanostructure. The induced average current (in the absence of bias), flows in the direction of the SAW wave vector,  $\mathbf{q}$ . A realistic treatment of the experimental geometry [39] only allowed a calculation at low SAW amplitude,  $P$ , yielding  $Q \propto P^2$ . The screening of the piezoelectric potential in the wide banks of the channel is also difficult to treat exactly. In view of this, we have proposed a simple model [38], in which the quantum channel is described by a finite one-dimensional tight-binding chain, whose on-site energies are modulated in time

$$\epsilon_n(t) = V + P \cos[\omega t - qa(n - n_0)]. \quad (19)$$

(Effects due to gradual screening, or reflections from the channel ends, can be incorporated as well [38].) Here  $V$  represents the gate voltage and  $P > 0$ , so that  $\epsilon_n$  has a maximum (minimum) in the center of the channel  $n_0 = (N + 1)/2$  at  $t = 0$  ( $T/2$ ). Within this simplified model, the charge pumped within each period of the modulating potential can be written as [38]

$$Q = \frac{eJ_L^2 \sin ka}{\pi J} \int_{-T/2}^{T/2} dt \sum_{n=1}^N \dot{\epsilon}_n |g_{n,1}|^2, \quad (20)$$

where  $J_L$  denotes the coupling of the finite chain to the leads,  $J$  is the tight-binding coupling on the leads,  $k$  is the wave vector of the incoming scattering state (corresponding to the Fermi energy), and  $g_{\ell,m}$  is the instantaneous Green function matrix of the finite chain, (with the coupling to the infinite leads included as a self-energy).

As has been found for the turnstile device in the previous section, the charge pumped by the SAW correlates with the behavior of the time-average transmission through the one-dimensional channel [38]: Wherever that transmission shows spikes, as function of the tight-binding parameters,  $Q$  exhibits large changes. The typical variation of  $Q/e$ , as function of the gate voltage  $V$ , is depicted in Fig. 3, demonstrating that a staircase structure, reminiscent of the one observed in the experiments [5], can result from interference effects alone.

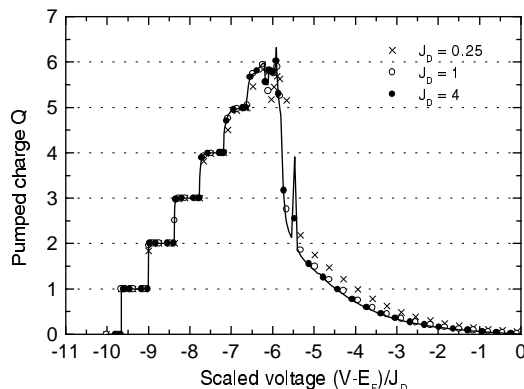


**Figure 3.** The pumped charge *vs.* the gate voltage, for a SAW wave length equal to 4 times the channel length.

Our simplified model allows for a detailed study of the robustness of the staircase structure against variation of the couplings to the leads, of the SAW amplitude  $P$ , of the Fermi energy, and other parameters. As an example, we portray in Fig. 4 the deterioration of the staircase structure upon increasing the coupling to the leads. That increase amounts to a broadening of the resonant levels within the channel, and consequently to the reduction of the quantization.

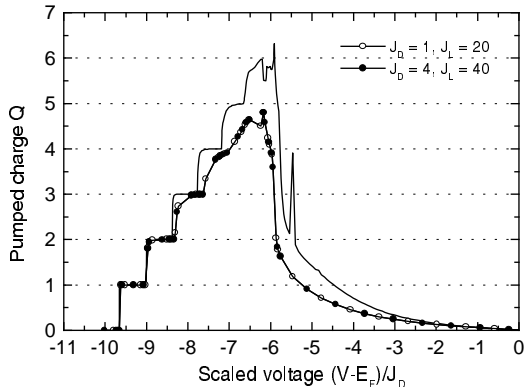


**Figure 4.** The deterioration of the staircase structure upon increasing the coupling to the leads (scaled by the tight-binding parameter  $J_L$ ).

The quantization is also stable with respect to a random noise in the channel, or a gradual screening of the SAW, as shown in Fig. 5. The shape and the interval between the steps may vary as the pumping potential is modified, but the  $Q(V)$  curve follows the same generic pattern as a function of the SAW amplitude  $P$ : the first step appears once a certain threshold value of  $P$  is exceeded, and the number of steps increases gradually as  $P$  is further elevated above the threshold.

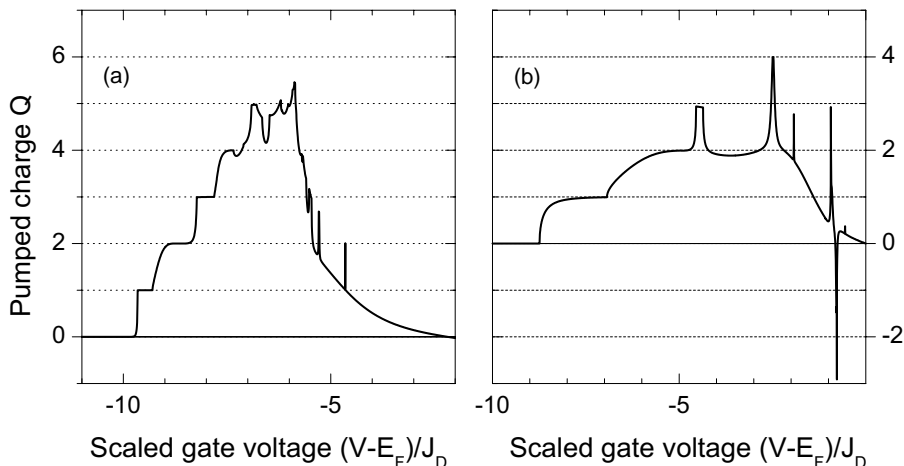


**Figure 5.** (a) The effect of a static disorder on the staircase structure. Random on-site energies  $V_n$ , drawn from a uniform distribution  $[-J_d, J_d]$  have been added to  $\epsilon_n$ . (b) Effects of SAW damping within the channel, modelled by multiplying the second term in Eq. (19) with a Gaussian profile,  $e^{-[a(n-n_0)/l_0]^2}$ ,  $l_0 = L/4$ .

Another interesting feature is that when the quantization is due to interference (as opposed to the Coulomb-blockade effect), the staircase structure appears also in the amplitude of the higher harmonics, as exemplified in Fig. 6.

To conclude this section, we note that even within this simple 1D model, it is possible to study effects



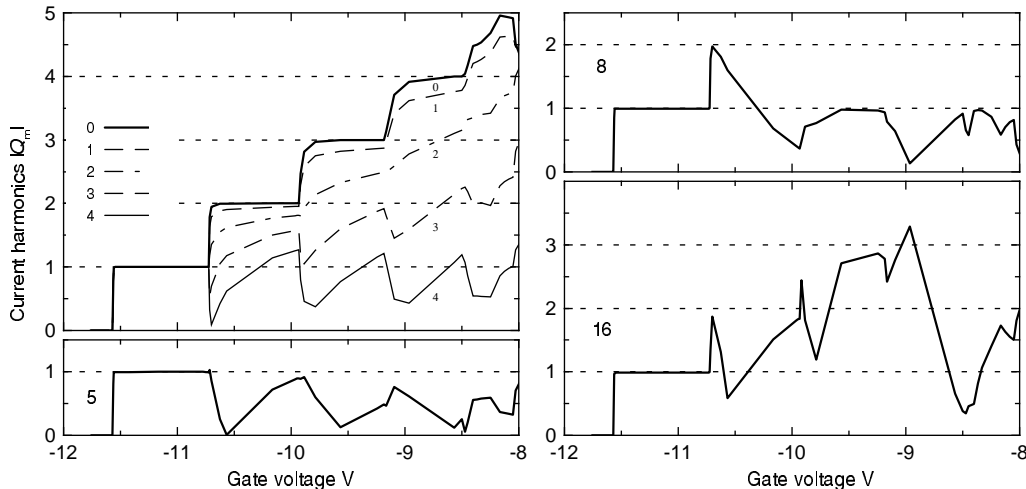


**Figure 6.** Higher harmonics of the pumped charge.

arising from variations of the SAW amplitude  $P$  in space (due to screening effects, or to multiple reflections from the channel's ends), or from random energies  $\{V_n\}$ , which may represent impurities within the channel.

## 5. Concluding remarks

Using simplified models, we have demonstrated that interference effects suffice to produce transfer of integral number of electrons through a mesoscopic (unbiased) system, subject to a periodically-varying potential. The calculations presented above utilize the expression for the pumped charge,  $Q$ , in the adiabatic approximation, that is, keeping only the first-order of the expansion (8). However, the next-order corrections need not be small; It is therefore an open question whether the quantization, and its relation to resonant transmission, will still be present when higher terms in the temporal expansion are retained. We hope to pursue these issues in the future.

## Acknowledgements

We thank Y. Imry, Y. Levinson, and P. Wölfle for helpful conversations. This research was carried out in a center of excellence supported by the Israel Science Foundation, and was supported in part by the Albert Einstein Minerva Center for Theoretical Physics at the Weizmann Institute of Science.

## References

- [1] D. J. Thouless, *Phys. Rev. B* **27** (1983) 6083.
- [2] Q. Niu and D. J. Thouless, *J. Phys. A* **17** (1984) 2453; Q. Niu, *Phys. Rev. Lett.* **64** (1990) 1812.
- [3] F. Hekking and Yu. V. Nazarov, *Phys. Rev. B* **44** (1991) 9110.
- [4] B. L. Altshuler and L. I. Glazman, *Science* **283** (1999) 1864.
- [5] J. M. Shilton, V. I. Talyanskii, M. Pepper, D. A. Ritchie, J. E. F. Frost, C. J. Ford, C. G. Smith and G. A. C. Jones, *J. Phys.: Condens. Matter* **8** (1996) L531; V. I. Talyanskii, J. M. Shilton, M. Pepper, C. G. Smith, C. J. Ford, E. H. Linfield, D. A. Ritchie, and G. A. C. Jones, *Phys. Rev. B* **56** (1997) 15180; V. I. Talyanskii, D. S. Novikov, B. D. Simons, and L. S. Levitov, *Phys. Rev. Lett.* **87** (2001) 276802; A. M. Robinson, V. I. Talyanskii, M. Pepper, J. E. Cunningham, E. H. Linfield, and D. A. Ritchie, *Phys. Rev. B* **56** (2002) 045313.

- [6] L. J. Geerligs, V. F. Anderegg, P. A. M. Holweg, J. E. Mooij, H. Pothier, D. Esteve, C. Urbina, and M. H. Devoret, *Phys. Rev. Lett.* **64** (1990) 2691.
- [7] L. P. Kouwenhoven, A. T. Johnson, N. C. van der Vaart, A. van der Enden, C. J. P. M. Harmans, and C. T. Foxon, *Z. Phys.* **B85** (1991) 381; *Phys. Rev. Lett.* **67** (1991) 1626; T. H. Oosterkamp, L. P. Kouwenhoven, A. E. A. Koolen, N. C. van der Vaart, and C. J. P. M. Harmans, *Phys. Rev. Lett.* **78** (1997) 1536.
- [8] H. Pothier, P. Lafarge, U. Urbina, D. Esteve and M. H. Devoret, *Europhys. Lett.* **17** (1992) 249.
- [9] B. L. Hazelzet, M. R. Wegewijs, T. H. Stoof, and Yu. V. Nazarov, *Phys. Rev. B* **63** (2001) 165313.
- [10] M. W. Keller, J. M. Martinis, N. M. Zimmerman, and A. H. Steinbach, *Appl. Phys. Lett.* **69** (1996) 1804; M. Covington, M. W. Keller, R. L. Kautz, and J. M. Martinis, *Phys. Rev. Lett.* **84** (2000) 5192.
- [11] B. Spivak, F. Zhou, and M. T. Beal-Monod, *Phys. Rev. B* **51** (1995) 13226.
- [12] P. W. Brouwer, *Phys. Rev. B* **58** (1998) R10135; *Phys. Rev. B* **63** (2001) 121303; M. L. Polianski and P. W. Brouwer, *Phys. Rev. B* **64** (2001) 075304.
- [13] F. Zhou, B. Spivak, and B. Altshuler, *Phys. Rev. Lett.* **82** (1999) 608.
- [14] T. A. Shutenko, I. L. Aleiner, and B. L. Altshuler, *Phys. Rev. B* **61** (2000) 10366.
- [15] S. H. Simon, *Phys. Rev. B* **61** (2000) R16327.
- [16] J. A. Avron, A. Elgart, G. M. Graf, and L. Sadun, *Phys. Rev. B* **62** (2000) R10618.
- [17] A. V. Andreev and A. Kamenev, *Phys. Rev. Lett.* **85** (2000) 1294.
- [18] I. L. Aleiner, B. L. Altshuler, and A. Kamenev, *Phys. Rev. B* **62** (2000) 10373.
- [19] Y. Wei, J. Wang, and H. Guo, *Phys. Rev. B* **62** (2000) 9947; Y. Wei, J. Wang, H. Guo, and C. Roland, *Phys. Rev. B* **64** (2001) 115321.
- [20] Y. Levinson, O. Entin-Wohlman, and P. Wölfle, *Physica A* **302** (2001) 335.
- [21] Y. Makhlin and A. D. Mirlin, *Phys. Rev. Lett.* **87** (2001) 276803.
- [22] M. G. Vavilov, V. Ambegaokar, and I. L. Aleiner, *Phys. Rev. B* **63** (2001) 195313.
- [23] D. Cohen, (2002) cond-mat 0208233.
- [24] M. Moskalets and M. Büttiker, *Phys. Rev. B* **64** (2001) 201305; *Phys. Rev. B* **66** (2002) 035306.
- [25] M. L. Polianski, M. G. Vavilov, and P. W. Brouwer, *Phys. Rev. B* **65** (2002) 245314.
- [26] J. N. H. J. Cremers and P. W. Brouwer, *Phys. Rev. B* **65** (2002) 115333.
- [27] M. Switkes, C. M. Marcus, K. Campman and A. C. Gossard, *Science* **283** (1999) 1905.
- [28] T. Aono, (2002) cond-mat 0205395.
- [29] E. R. Mucciolo, C. Chamon, and C. M. Marcus, *Phys. Rev. Lett.* **89** (2002) 146802.
- [30] O. Entin-Wohlman and A. Aharony, *Phys. Rev. B* **66** (2002) 035329.
- [31] O. Entin-Wohlman, A. Aharony, and Y. Levinson, *Phys. Rev. B* **65** (2002) 195411.
- [32] M. Büttiker, H. Thomas, and A. Prêtre, *Z. Phys. B* **94** (1994) 133.
- [33] Y. Levinson and P. Wölfle, *Phys. Rev. Lett.* **83** (1999) 1399.
- [34] Y. Levinson, *Phys. Rev. B* **61** (2000) 4748.
- [35] E. Akkerman, *J. Math. Phys.* **38** (1997) 1781.
- [36] M. Muskalets and M. Büttiker, *Phys. Rev. B* **66** (2002) 205320.

- [37] M. Wagner, *Phys. Rev. A* **51** (1995) 798.
- [38] A. Aharony and O. Entin-Wohlman, *Phys. Rev. B* **65** (2002 ) 241401; O. Entin-Wohlman, A. Aharony, and V. Kashcheyevs, *J. Phys. Soc. Japan* **72** (2003) Supp. A 77.
- [39] Y. Levinson, O. Entin-Wohlman, and P. Wölfle, *Phys. Rev. Lett.* **85** (2000) 634.